NONLINEAR EFFECTS AND POSSIBLE TEMPERATURE INCREASES IN ULTRASONIC MICROSCOPY

J. WÓJCIK, J. LITNIEWSKI, L. FILIPCZYŃSKI and T. KUJAWSKA

Institute of Fundamental Technological Research, Polish Academy of Sciences,
Department of Ultrasound,
00-049 Warszawa, Świętokrzyska 21, Poland
E-mail: jwojcik@ippt.gov.pl

Visualisation of living tissues or cells at a microscopic resolution provides a foundation for many new medical and biological applications. Propagation of waves in ultrasonic microscopy is a complex problem due to finite amplitude distortions. Therefore, to describe it quantitatively, a numerical model developed by the first author was applied. The scanning acoustic microscope operating at 34 MHz was used with strongly focused ultrasonic pulses of 4 periods. For measurements of signals, a 100 MHz PVDF probe was constructed. Its frequency characteristic was found experimentally. The numerical calculation procedure for nonlinear propagation was based on previous papers of the authors. Computations have shown that in the case under consideration, only the spectrum with an input lens pressure amplitude of 1 MPa was in agreement with the experimental one. Based on transducer power measurements, a slightly smaller pressure value was obtained thus confirming, to a good approximation, the correctness of the applied methods. A significant parameter is the ratio of the amplitudes of the second to the first calculated harmonics, which shows the extent of the nonlinearity. In our case it was equal to 0.5. After averaging over the surface of the finite electrode size used in measurements, this ratio was reduced to 0.2. Pressure distributions in the lens cavity and the following region in water were computed for the first 4 harmonics making it possible to determine many features of the nonlinear propagation effects in the microscope. Using the thermal conductivity equation and the rate of heat generation per unit volume, determined for nonlinear propagation in water, a focal temperature increase of 3.3° C was obtained. It was computed for a repetition frequency of 100 kHz. The computed temperature increases can be significant and also harmful, especially when imaging small superficial structures and testing living cell cultures. However, they can be easily decreased by reducing the repetition frequency of the microscope. The developed numerical procedure can be applied for much higher frequencies when living cells in culture are being investigated.

1. Introduction

An extensive overview of medical and biological applications at the microscopic resolution was given by FOSTER et al. [2000]. For example, a wide use of high frequency technique was demonstrated in ophthalmology for visualisation of the anterior chamber of eye, as well as in dermatology [NOWICKI et al., 1996], where it is possible to differentiate the skin tumors. Recently even monitoring of morphea and lichen sclerosus et atrophicus (LSA) [SZYMAŃSKA et al. 2000] has been reported.

The quantitative use of ultrasonic microscopy in living cells in culture was shown by LITNIEWSKI and BREITER-HAHN [1990] at a frequency of 1 GHz where values of the acoustic impedances and attenuation coefficients in the cell periphery, and near to its central part were determined. Nowadays biomicroscopy has become a promising field of growing interest and great potential importance. In all such applications the possible temperature increase should be avoided to eliminate its destructive influence in the cells. Ultrasonic microscopes have found a wide application also in material investigations [BRIGGS, 1992].

Propagation of acoustic waves in ultrasonic microscopy is a complex problem due to finite amplitude distortions. Nonlinear effects produced by strongly focused beams with half- angle apertures exceeding 16° cannot be described by simplified theories based on the paraxial approximation [TJOTTA et al. 1991]. Also diffraction effects and the high absorption of the liquids involved should be considered. Therefore a numerical model developed by the first author was applied [FILIPCZYŃSKI et al. 1999, see pp. 290–292].

In the present paper we show by means of numerical and experimental methods the effects of high nonlinearity being an important, and in many cases - a decisive factor in ultrasonic microscopy. Also demonstrated are some potential dangers for biological applications caused by temperature increases.

2. Experimental determination of higher harmonics

The scanning acoustic microscope (SAM) operating at 34 MHz [LITNIEWSKI, 2001] was used as a source of strongly focused ultrasonic waves (Fig. 1). Acoustic pulses
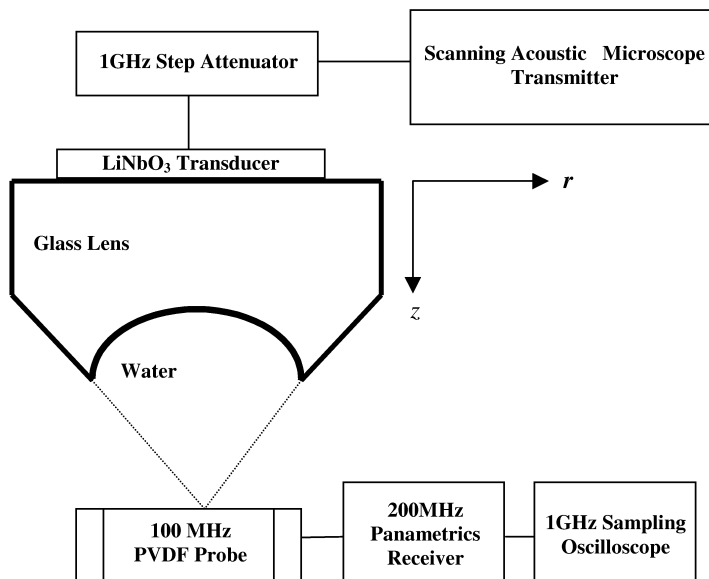

Fig. 1. Scanning acoustic microscope with the measurement system.

of 4 periods (duration time of 0.12 µs) were focused in water by a glass spherical lens with a radius of 2.54 mm and the aperture half-angle of 50°. The pulse length was chosen in this way to obtain a well defined fundamental frequency. The lens cavity was situated near to the transition zone of the near and far fields of a circular $LiNBO_3$ transducer, 4.4 mm in diameter, assuring a smooth, resembling a Gaussian, distribution of the acoustic pressure on the lens surface (Fig. 2).
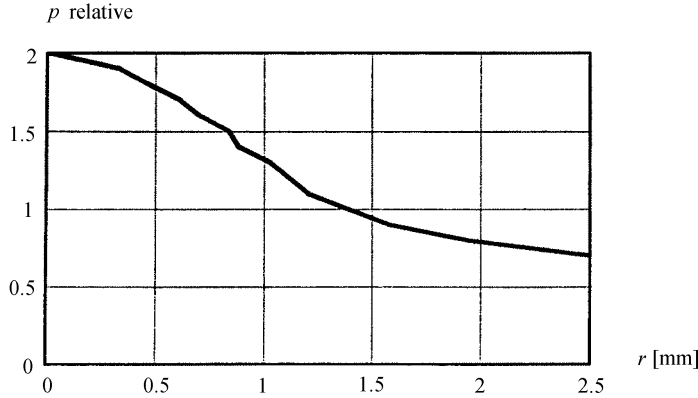

Fig. 2. Pulse pressure distribution computed in the glass medium along the coordinate r perpendicular to the direction z of the symmetry axis for which $r = 0$. The distance from the transducer surface was equal to 30 mm and the pressure at the transducer surface was assumed to be 1.

For measurement of the signals transmitted by the SAM, a special 100 MHz PVDF probe, P_{100}, was constructed with an active electrode diameter of 1 mm. The frequency characteristic of the probe was found by recording first the probe response to an input pulse $f_i(t)$ in the form of a short electric pulse shown in Fig. 3. It was generated by the Panametrics Pulsar /Receiver (model 5900 PR) with a rise time of 4 ns/100 V. The amplitude spectrum of this pulse $S(f_i)$ is presented also in Fig. 3. This and subsequent spectra were calculated by means of the Mathcad 2001 procedure.

The acoustic pulse $f_0(t)$ emitted by the probe P_{100} was back-reflected by a sapphire flat reflector situated in water 2 mm distant from the probe. Then it was detected by the same probe P_{100}, amplified by the wide-band Panametric amplifier, time averaged for noise reduction, and digitized and stored in the digital oscilloscope (HP 54810A, 1 GHz). The reflected pulse $f_r(t)$ received in this way is shown in Fig. 4, as well as its amplitude spectrum $S(f_r)$ compensated for absorption in water. The spectrum of this pulse was changed twice by the transfer function $H(\omega)$ of the probe P_{100} [DIEULESAINT and ROYER, 1974].

The first time it was changed when transforming the spectrum of the input pulse $S(f_i)$ into the spectrum of the output acoustic pulse $S(f_o)$, and the second time, when receiving the back reflected acoustic pulse and transforming it into the electric pulse $f_r(t)$ with spectrum $S(f_r)$.
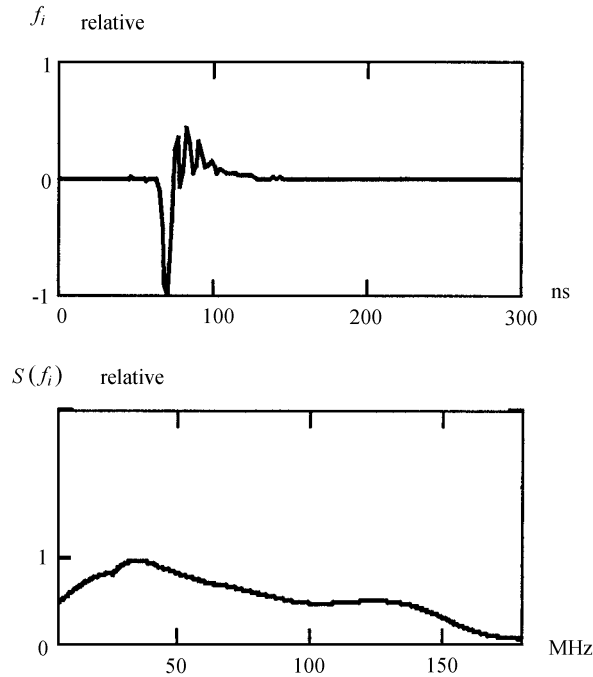
Fig. 3. Input pulse $f_i(t)$ applied to the 100 MHz probe (top) and its normalized amplitude spectrum $S(f_i)$ in linear scale (bottom).

Thus the obtained amplitude spectra — $S(f_i)$ of the input function and $S(f_r)$ of the reflected pulse — were connected by the relation

$$S(f_r) = S(f_i) \cdot H(\omega)^2. \tag{1}$$

Hence finally, the transfer function $H(\omega)$, or in other words, the frequency characteristic function of the probe P_{100}, was obtained as presented in Fig. 5. It demonstrates an almost constant sensitivity in the frequency range $(-3$ dB$)$ from 50 MHz up to 135 MHz. In the case under consideration, a reasonable supposition was made assuming the same value of the transfer function $H(\omega)$ for both the transmitted and received pulses.

The described probe was placed in the vicinity of the focal region of the lens. After wide-band amplification, the signals detected by the probe were sampled and stored in the digital oscilloscope (Fig. 1). The measured spectrum was compensated for the frequency characteristic of the probe P_{100} (Fig. 5).

3. Numerical method

For numerical determination of the pressure distributions a procedure based on Fourier series was applied. A plane boundary pulse was transformed by a concave spherical lens to a focused ultrasonic beam. The basis and details of this procedure were described
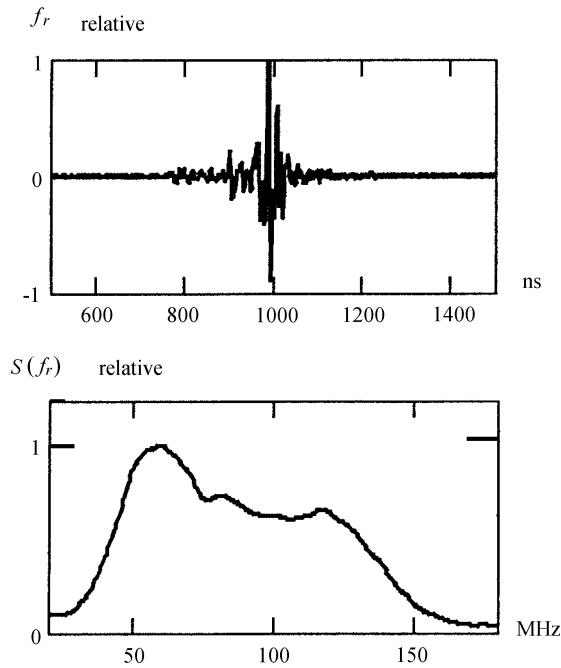
f_r relative

Fig. 4. Pulse $f_r(t)$ obtained by the 100 MHz probe due to back-reflection in water from a sapphire reflector (top), and its amplitude spectrum $S(f_r)$ in linear scale compensated for absorption in water (bottom).
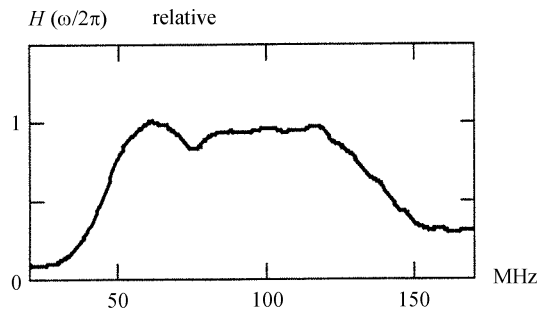

Fig. 5. Frequency characteristic function of the probe showing a constant sensitivity (-3 dB) in the frequency range from 50 MHz up to 135 MHz (in linear scale).

in a previous paper by WÓJCIK [1998, 1999]. It was based on the nonlinear propagation procedure of CHRISTOPHER and PARKER [1991], then it was verified experimentally [FILIPCZYŃSKI et al., 1999] and justified mathematically [WÓJCIK, 2000]. In the glass which was directly coupled with the transducer, linear numerical methods were used based on typical formulae valid for solid media [KRAUTKRAMMER, 1990] with longitudinal and transverse wave speeds of 5900 m/s and 3600 m/s, while absorption was neglected.

In the lens cavity and in the following region which was filled with water, a nonlinear numerical procedure was necessary due to the nonlinear properties of water and to the very high pressure amplitudes. Also absorption effects had to be taken into account.

For temperature increases the following thermal conductivity equation [NYBORG, 1988] was utilised:

$$\frac{\partial T}{\partial t} = \kappa \nabla^2 T + \frac{Q}{c_s \rho}\,, \tag{2}$$

where T — ambient temperature, t — time, κ – coefficient of thermal conductivity, c_s – specific heat, ρ – density, ∇^2 – Laplacean operator, Q – rate of heat generation per unit volume (power density of heat sources).

The rate Q of the relation (2) can be expressed in cylindrical coordinates where $x = (z, r)$ due to axial symmetry of the problem. In this case the nonlinear propagation is taken into account and then [WˇJCIK $et\ al.$, 1999]

$$Q(\mathbf{x}) = \frac{p_p^2}{\rho c} \sum_{n=1}^{N} a(n)|C_n(\mathbf{x})|^2 \tag{3}$$

here p_p denotes the peak positive pressure in the pulse, ρc – acoustic impedance of the medium, N – the number of harmonics, $a(n) = \alpha_l (f_r)^l n^l$ – coefficient of absorption, α_l – absorption parameter, f_r – repetition frequency, l – power of the absorption dependence on frequency, $C_n(x)$ – component of the Fourier spectrum of the pulse under investigation, $x = (z, r)$ – coordinates of the cylindrical system.

At the lens glass-water boundary a perfect thermal isolation was assumed. Solving numerically Eq. (2) the axial distribution of the temperature increase and its maximum value in water for the repetition frequency of 100 kHz was computed. A similar technique as in the previous paper [WÓJCIK $et\ al.$ 1999] was used.

4. Assessment of the supplied power and the generated pressure

The radiating circular LiNBO$_3$ transducer was loaded by glass on one side only. Its electrical input admittance was measured to be A = $(20 + \text{j}0.14)$ mS. The admittance was determined by means of an admittance bridge. The spherical lens at the end of the glass cylinder decreased to a great extent the possible back reflection of the plane wave, thus reducing standing waves. In this way it was possible to carry out measurements on the pulses used. Since the voltage of the electrical driving pulse was equal to 30 V$_{\text{pp}}$, we obtained the supplied power of 2.25 W.

Knowing the supplied power and the transducer diameter, the average intensity could be determined and hence also the corresponding average pressure at the transducer surface. Linear numerical computations of the radiated pulse beam in the glass cylinder have shown that the axial pressure at its end, at a distance of 30 mm, was twice as great as that at the transducer surface (Fig. 2). Attenuation in glass was negligibly small. Finally, after penetration of the glass-water boundary, the lens output axial pressure at the boundary in water reached a value of $P_2 = 0.79$ MPa (see Table 1).

Table 1. Estimation of the output lens pressure P_2 in water

Voltage of the electrical driving pulse	V_{pp}	30
Measured transducer admittance	mS	$20 + j\,0.14$
Power supplied to the transducer	W	2.25
Transducer area (diameter 4.4 mm)	mm^2	15.2
Intensity I at the transducer surface	MW/m^2	0.148
Corresponding pressure $p = \sqrt{2 \cdot \rho_G c_G \cdot I}$	MPa	2.01
Double higher axial pressure at the lens input** $2p$	MPa	4.02
Lens output axial pressure* $P_2 = 4p\rho_W c_W / (\rho_G c_G + \rho_W c_W)$	MPa	0.79

* For glass $\rho_G c_G = 13.7$ MRayl, for water $\rho_W c_W = 1.5$ MRayl
** See Fig. 2

Table 2. Numerical and experimental pressure amplitudes of first 5 harmonics (after normalization)

No of harmonic	1	2	3	4	5
Numerical amplitudes (after averaging over the measuring electrode)	1	0.20	0.088	0.053	0.030
Experimental amplitudes	1	0.2	0.088	0.064	0.035

Computations were performed at first for various pulse pressures causing nonlinear propagation. Finally a pressure amplitude of $P_1 = 1$ MPa at the axis of the output of the spherical lens was found to match the numerical spectrum with the experimental one as shown in Table 2. The amplitude spectra of the acoustic pulses in the focal region were calculated and compared with the pulse spectrum obtained experimentally, reaching agreement only for a pressure value of $P_1 = 1$ MPa, which was a little higher than the value of $P_2 = 0.79$ MPa (by 2 dB) (see Table 1).

5. Computations and experimental results

The computed spectrum (Fig. 6) shows in the focus a very high number of harmonics up to 1120 MHz. This result can not be directly used in the real microscope due to its limited receiving band and unknown signal-to-noise ratio. A much more significant parameter, showing the range of potential possibilities of harmonic generation, is the spectral amplitude ratio of the second to the first harmonics, $p_{2/1}$.

This ratio obtained numerically was equal to $p_{2/1} = 0.5$ (-6.0 dB) (Fig. 6). However, to compare the numerical and experimental results, the numerical ones had to be averaged over the surface of the electrode of the probe, P_{100}, used in measurements of the spectrum.
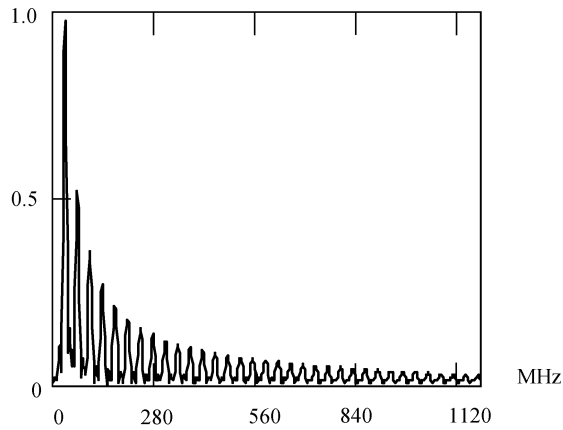
Fig. 6. Spectrum computed in the focus.

For this purpose the computed transverse pressure distributions in the beam were used. Those results were obtained previously [WÓJCIK *et al.*, 2001, Figs. 3 and 4]. The numerical spectrum averaged in this way is shown in Table 2 to be in a good agreement with experiment up to the 5-th harmonic. It is interesting to notice that even at so small a radiated acoustic power as 2.25 W, we obtained very high nonlinearity in the focus in water represented by the spectral ratio $p_2/p_1 = 0.5$ (Fig. 6). However, after taking into account the experimental spectrum which was measured with a finite electrode size, after averaging over the electrode size, this ratio was smaller and equal to $p_2/p_1 = 0.2$ (-14 dB) (Table 2). On the other hand, GERMAIN and CHEEKE [1988, Fig. 4] obtained a power ratio of -20 dB corresponding only to $p_2/p_1 = 0.1$ at the very high lens output power of 100 W.

The difference of the above results may be caused by such reasons as the physical size of the measuring electrodes, and by the differing geometry of the acoustic lens producing different gains etc. In our case the ratio of the computed maximum pressure in the focus, p_f, to the lens output pressure, p_o ($= P_1$) was equal to $p_f/p_o = 49$.

6. Discussion and conclusions

The nonlinear numerical procedure applied here for the acoustic microscope made it possible to determine exactly the field distributions of strongly focused beams in the lens cavity and in the following region. Similar pressure values of $P_1 = 1$ MPa obtained by spectrum matching between experimental and computed results, and by direct transducer measurement, giving $P_2 = 0.79$ MPa, seems to confirm to a good approximation the correctness of the applied procedure. This positive result was obtained in spite of many simplifying assumptions which were necessary to carry out the comparison. Finally the spectrum obtained for the axial pressure amplitude of 1 MPa at the output of the lens was found to match the experimental one (Table 2).

As the nonlinearity measure of the microscope, the ratio of the amplitudes of the second and first harmonics should be considered for characterizing the possibility of the generation of higher harmonics.

Pressure distributions in the lens focal region filled with water were presented for the first 4 harmonics (Fig. 7). The computed values of the focal pressure spectrum are shown in Fig. 6 for all the harmonics. The obtained results can be easily expanded for higher harmonics by means of the method used here. Thus it is possible to determine many interesting data concerning effective focal cross-sections, intensity distributions, pulse shape deformations, determination of local attenuation, and of the power density of heat sources, thus providing a description of nonlinear propagation effects in the microscope that were previously lacking.
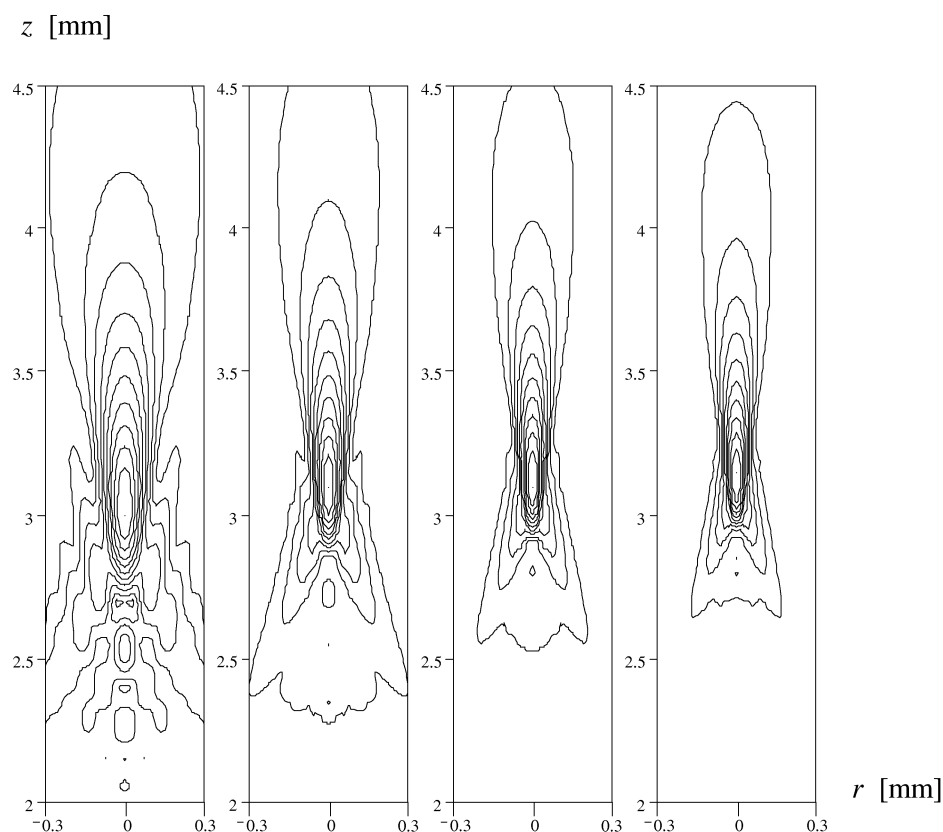
z [mm]

r [mm]

Fig. 7. Pressure distributions computed for the first (from left to right), second, third and fourth harmonics. All scales in mm, steps of constant pressure contours equal to 0.1 of the maximum pressure.

Also in the case of nonlinear propagation, temperature increases along the lens axis were determined by means of the numerical procedure. The temperature increase depends on many factors such as the local intensity, its duration, its repetition frequency, the kind

of the tissue, its attenuation and on the nonlinear parameter B/A. To obtain a general view of the temperature effect, we assumed the medium to be water and the focal pressure amplitude as obtained above, namely $p_f = 49$ MPa with a pulse duration of 0.12 µs. The maximum range of the microscope was equal to 7.5 mm in water. Hence the repetition frequency can be as high as 100 kHz. For these conditions the maximum computed temperature increase was $\Delta T = 3.3°$C. Its axial distribution is presented in Fig. 8.

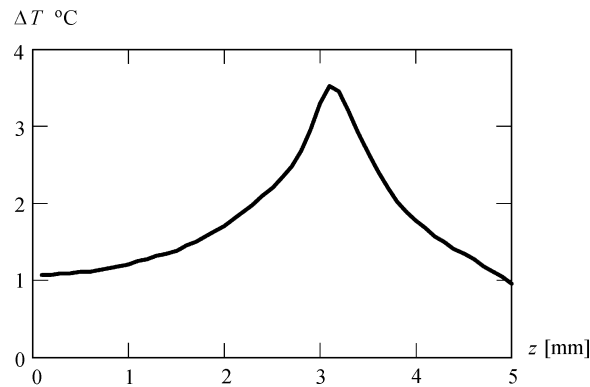Fig. 8. Axial distribution of the temperature increase ΔT computed in water.

The computed temperature increases can be in some cases be significant and also harmful, especially when testing superficial structures. However, the temperature increase in the pulse mode is proportional to the repetition frequency so, for example, in the case under consideration it decreases in water at a repetition frequency of 10 kHz to a value of only $\Delta T = 0.33°$C.

The developed numerical procedure can be expanded for much higher frequencies when living cells in culture are being investigated.

Acknowledgments

References

[1] A. BRIGGS, *Acoustic microscopy*, Oxford Science Publishers, Clarendon Press, 1992.

[2] P. CHRISTOPHER and K. PARKER, *New approaches to nonlinear diffractive field propagation*, J. Acoust. Soc. Am., **90**, 488–400 (1991).

[3] E. DIEULESAINT and D. ROYER, *Ondes elastiques dans les solides*, Masson et Cie., Paris 1974, pp. 35,36 (See also English translation: Elastic waves in solids, J. Wiley, New York 1974).

[4] F. DUCK, *Physical properties of tissue*, London, Academic Press, 1990, pp. 98, 108

[5] L. FILIPCZYŃSKI, T. KUJAWSKA, R. TYMKIEWICZ and J. WÓJCIK, *Nonlinear and linear propagation of diagnostic ultrasound pulses*, Ultrasound in Med. & Biol., **25**, 285–299 (1999).

[6] F. FOSTER, C. PAVLIN, K. HARASIEWICZ, D. CHRISTOPHER and D. TURNULL, *Advances in ultrasound biomicroscopy*, Ultrasound in Med. and Biol., **26**, 1–27 (2000).

[7] L. GERMAIN and J. CHEEKE, *Generation and detection of high-order harmonics in liquids using a scanning acoustic microscope*, J. Acoust. Soc. Am., **83**, 942–949 (1988).

[8] J. KRAUTKRAMMER and H., *Ultrasonic testing of materials*, Springer, Berlin 1990.

[9] J. LITNIEWSKI, J. BEREITER-HAHN, *Measurements of cells in culture by scanning acoustic microscopy*, Journal of Microscopy, **158**, 1, 95–107 (1990).

[10] J. LITNIEWSKI, *An acoustic microscope for microflaw inspection and subsurface imaging*, Archives of Acoustics, **26**, 1 (2001).

[11] A. NOWICKI, J. LITNIEWSKI, J. LIWSKI, W. SECOMSKI, P. KARLOWICZ and M. LEWANDOWSKI, *Superficial tissue microsonography, Acoustical imaging*, Plenum Press, New York, **22**, 501–505 (1996).

[12] W. NYBORG, *Solutions of the bio-heat transfer equation*, Phys. Med. Biol., **33**, 785–792 (1988).

[13] G. SZYMAŃSKA, A. NOWICKI, K. MLOSEK, J. LITNIEWSKI, M. LEWANDOWSKI, W. SECOMSKI and R. TYMKIEWICZ, *Skin imaging with high frequency ultrasound*, Europ. J. Ultrasound, **12**, 9–16 (2000)

[14] J. TJOTTA, S. TJOTTA and E. VEFRING, *Effects of focusing on the nonlinear interaction between two collinear finite amplitude sound beams*, J. Acoust. Soc. Am., **89**, 1017–1027 (1991).

[15] J. WÓJCIK, *Conservation of energy and absorption in acoustic fields for linear and nonlinear propagation*, J. Acoust. Soc. Am., **104** (5), 2654–2663 (1998).

[16] L. WÓJCIK, J. LITNIEWSKI, L. FILIPCZYŃSKI, *Numerical and experimental determination of high nonlinearities in ultrasonic microscopy*, Proceedings of the 17th International Congress on Acoustics, Rome 2001, Paper 7B.02.02, pp 1–2.

[17] J. WÓJCIK, *A new theoretical basis for numerical simulations of nonlinear acoustic fields*, Proceedings of the 15th International Symposium on Nonlinear Acoustics, Goettingen 1999, American Society of Physics, **524**, 141–144 (2000).

[18] J. WOJCIK, L. FILIPCZYNSKI and T. KUJAWSKA, *Temperature elevations computed for three layer and four layer obstetrical tissue models in nonlinear and linear propagation cases*, Ultrasound in Med. and Biol., **25**, 259–267 (1999).